Size-selective opening of the blood–brain barrier by targeting endothelial sphingosine 1–phosphate receptor 1

Keisuke Yanagida[a,b,c,1], Catherine H. Liu[c,1], Giuseppe Faraco[d], Sylvain Galvani[a,b], Helen K. Smith[c], Nathalie Burg[c], Josef Anrather[d], Teresa Sanchez[c], Costantino Iadecola[d], and Timothy Hla[a,b,c,2]

[a]Vascular Biology Program, Boston Children's Hospital, Boston, MA 20115; [b]Department of Surgery, Harvard Medical School, Boston, MA 20115; [c]Center for Vascular Biology, Department of Pathology and Laboratory Medicine, Weill Cornell Medicine, New York, NY 10065; and [d]Feil Family Brain and Mind Research Institute, Weill Cornell Medicine, New York, NY 10065

Edited by Jason G. Cyster, University of California, San Francisco, CA, and approved March 14, 2017 (received for review November 10, 2016)

The vasculature of the central nervous system (CNS) forms a selective barrier termed the blood–brain barrier (BBB). Disruption of the BBB may contribute to various CNS diseases. Conversely, the intact BBB restricts efficient penetration of CNS-targeted drugs. Here, we report the BBB-regulatory role of endothelial sphingosine 1–phosphate (S1P) receptor-1, a G protein-coupled receptor known to promote the barrier function in peripheral vessels. Endothelial-specific *S1pr1* knockout mice (*S1pr1*^{iECKO}) showed BBB breach for small-molecular-mass fluorescence tracers (<3 kDa), but not larger tracers (>10 kDa). Chronic BBB leakiness was associated with cognitive impairment, as assessed by the novel object recognition test, but not signs of brain inflammation. Brain microvessels of *S1pr1*^{iECKO} mice showed altered subcellular distribution of tight junctional proteins. Pharmacological inhibition of $S1P_1$ function led to transient BBB breach. These data suggest that brain endothelial $S1P_1$ maintain the BBB by regulating the proper localization of tight junction proteins and raise the possibility that endothelial $S1P_1$ inhibition may be a strategy for transient BBB opening and delivery of small molecules into the CNS.

blood–brain barrier | sphingosine 1–phosphate | endothelium | tight junction | drug delivery

The blood–brain barrier (BBB) is a protective and regulatory interface that allows the entry of essential nutrients, while preventing harmful substances from entering the central nervous system (CNS) (1). BBB endothelial cells (ECs) contain abundant tight junction (TJ) proteins, which generate a paracellular seal. In addition, paucity of endocytotic vesicles in brain ECs results in low rates of transcytosis. Furthermore, brain ECs allow efficient transport of select molecules, such as glucose and amino acids, into the CNS (2). The capillary endothelium is surrounded by a defined basement membrane, pericytes, and astrocytic end-feet processes, constituting the neurovascular unit (NVU), which is essential for maintaining the homeostasis of the CNS (3). Disruption of the BBB is associated with various CNS diseases, including multiple sclerosis (MS), Alzheimer's disease (AD), and ischemic stroke (1–3). Conversely, in the normal state, the BBB hinders pharmacotherapy of CNS diseases by limiting drug delivery (4). Among the 7,000 drugs analyzed in the Comprehensive Medical Chemistry database, only 5% showed efficient BBB permeability allowing transport into the CNS (5). Therefore, novel approaches for a regulated opening of the BBB may be desirable to facilitate efficient pharmacotherapy of CNS diseases.

Sphingosine 1–phosphate (S1P), a pleiotropic lipid mediator, interacts with five G protein-coupled receptors (GPCRs), $S1P_{1–5}$, to regulate cell migration, adhesion, survival, and proliferation (6). Recently, an $S1P_1$ modulator, FTY720 (fingolimod), was approved as the first-line oral drug for relapsing–remitting MS (7). Furthermore, S1P and its prototypic receptor $S1P_1$ have been implicated in neurovascular diseases such as AD and ischemic stroke (8, 9). S1P activation of EC $S1P_1$ is essential for vascular development and barrier function (10). $S1P_1$ regulates G_i-dependent Rac activation, cytoskeletal reorganization, adherens junction (AJ) assembly, and focal adhesion formation, all of which are needed for enhancement of vascular barrier function (10). Indeed, genetic and pharmacological inhibition of $S1P_1$ increased vascular permeability in various organs such as lung, retina, and colon (11–14). However, the role of EC $S1P_1$ in CNS vasculature is unknown.

Here, we investigated the involvement of endothelial $S1P_1$ in BBB integrity in vivo using EC-specific *S1pr1* knockout mice (referred to as *S1pr1*^{iECKO} mice). The results demonstrate that brain endothelial $S1P_1$ regulates BBB integrity in a size-dependent manner. With protracted BBB leakiness, EC-specific *S1pr1* knockout mice displayed cognitive impairment, but no sign of brain inflammation. Biochemical analysis on brain microvessels revealed that subcellular localization of TJ proteins was altered in *S1pr1*^{iECKO} mice, which provides a molecular explanation for the size-selective BBB leakiness in these mice. Transient pharmacological inhibition of $S1P_1$ led to increased CNS penetration of small molecules, suggesting that targeting $S1P_1$ may be a promising strategy for the safe delivery of therapeutic agents into the CNS.

Results

Size-Selective BBB Opening in *S1pr1*^{iECKO} Mice. To assess the role of endothelial $S1P_1$ in brain vasculature, we used a mouse model in which $S1P_1$ is deleted in an EC-specific manner (*S1pr1*$^{flox/flox}$

Significance

The blood–brain barrier (BBB) poses a major obstacle for drug delivery to the central nervous system (CNS). This study revealed that genetic or pharmacological targeting of sphingosine 1–phosphate receptor-1 ($S1P_1$) facilitates a small-molecule-selective BBB opening, without major signs of CNS inflammation or injury. This size-selective BBB opening could be attributed to changes in the cytoskeletal association of tight junction proteins. Importantly, BBB opening by pharmacological blockage of $S1P_1$ was reversible, suggesting that targeting $S1P_1$ may be a promising strategy for the safe delivery of therapeutic agents into the CNS to treat neurodegenerative and neuroinflammatory diseases and neurological cancers.

Author contributions: K.Y., C.H.L., J.A., T.S., C.I., and T.H. designed research; K.Y., C.H.L., G.F., S.G., H.K.S., and N.B. performed research; K.Y., C.H.L., G.F., S.G., J.A., T.S., C.I., and T.H. analyzed data; and K.Y. and T.H. wrote the paper.

The authors declare no conflict of interest.

This article is a PNAS Direct Submission.

Freely available online through the PNAS open access option.

[1]K.Y. and C.H.L. contributed equally to this work.

[2]To whom correspondence should be addressed. Email: timothy.hla@childrens.harvard.edu.

This article contains supporting information online at www.pnas.org/lookup/suppl/doi:10.1073/pnas.1618659114/-/DCSupplemental.

Cdh5–Cre–ER^{T2}; referred to as *S1pr1*^{iECKO}) (12, 15–17). Mice were treated with tamoxifen for the first 3 d after birth and allowed to develop into adulthood. Quantitative PCR (qPCR) analysis of RNA from adult brain ECs showed >95% reduction of *S1pr1* expression (Fig. S1*A*). Brain ECs did not show compensatory up-regulation of *S1pr2* and *S1pr3* (Fig. S1*A*).

To address the role of endothelial $S1P_1$ in BBB function, we injected 1-kDa fluorescent tracer, Alexa Fluor 555–cadaverine, and examined its distribution in brain. As shown in Fig. 1*A*, *S1pr1*^{iECKO} brains showed enhanced tracer accumulation in the parenchyma by approximately fivefold compared with control mice (Fig. 1*B*), suggesting that CNS vasculature is leaky. The tracer accumulation into brain parenchyma was also observed when a 3-kDa dextran–tetramethylrhodamine (TMR) was administered (Fig. 1*C*). However, when the mice were injected with 10- and 70-kDa dextran–TMR, there was no significant difference in tracer accumulation between control and *S1pr1*^{iECKO} brains (Fig. 1 *D* and *E*). The blood–retina barrier, which is similar to the BBB, is tight and restrictive (18). Similar to brain, the enhanced leakage of 3-kDa dextran–TMR was also observed in *S1pr1*^{iECKO} retinas (Fig. S2).

CNS vasculature undergoes angiogenesis and remodeling at early postnatal stages (19, 20), alterations of which can affect subsequent BBB properties (2, 21). To determine whether $S1P_1$ regulates the BBB directly or indirectly via vascular developmental defects (2, 21), we deleted endothelial *S1pr1* in adult mice (>8 wk) and analyzed them for BBB function 4 wk after gene deletion. As in the case of early postnatal deletion, adult deletion of *S1pr1* enhanced BBB permeability to the 1-kDa Alexa Fluor 555–cadaverine by approximately fourfold (Fig. 1*F*). Collectively, these results indicate that endothelial $S1P_1$ directly regulates BBB integrity in a size-selective manner.

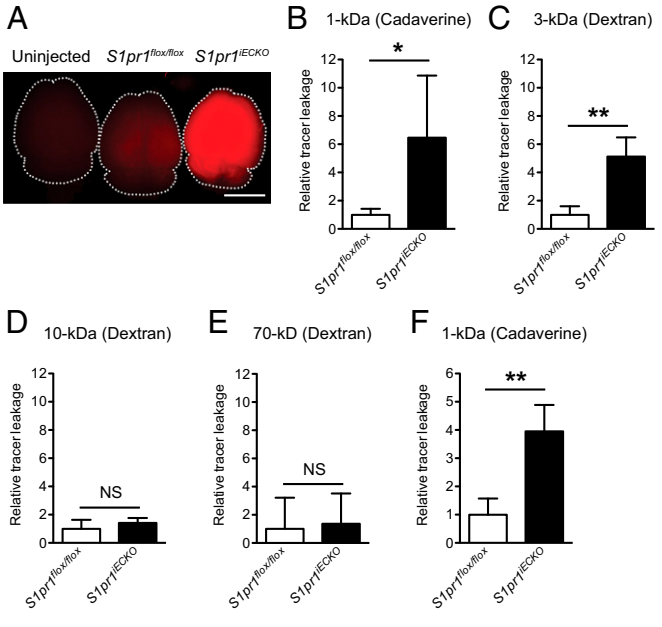

Fig. 1. Tracer extravasation into the brain is increased in *S1pr1*^{iECKO} mice. *S1pr1* deletion was induced after birth in *A–E* and in the adult in *F*. (*A*) Whole brain images taken after injection of 1-kDa Alexa Fluor 555–cadaverine. (Scale bar: 5 mm.) (*B–E*) Quantification of extravasated 1-kDa Alexa Fluor 555–cadaverine (*B*), 3-kDa dextran–TMR (*C*), 10-kDa dextran–TMR (*D*), and 70-kDa dextran–TMR (*E*) in control (*S1pr1*$^{flox/flox}$) and *S1pr1*^{iECKO} mice ($n = 3$ or 4). (*F*) Quantification of extravasated cadaverine in control and *S1pr1*^{iECKO} mice when the deletion was induced in the adult ($n = 3$). Data are expressed as mean ± SD. *$P < 0.05$; **$P < 0.01$ (Student's *t* test). NS, nonsignificant.

Normal Brain Vascular Structure in *S1pr1*^{iECKO} Mice. Because $S1P_1$ is a key regulator of sprouting angiogenesis (12, 22, 23), we next examined whether deletion of endothelial *S1pr1* affects CNS vascular development, maturation, and pattern formation. No abnormalities were detected in brain vascular density, diameter, and branch points in *S1pr1*^{iECKO} mice (Fig. 2 *A* and *B*). Because endothelial $S1P_1$ regulates pericyte investment during embryonic development (24), we assessed pericyte coverage in *S1pr1*^{iECKO} brain vasculature. Immunohistochemical staining with the pericyte marker CD13 did not show any anomalies in pericyte coverage or positioning relative to the ECs of the capillary wall (Fig. 2 *A* and *B*). Expression of pan-EC marker genes such as *Pecam1* and *Tek* in whole cortical or hippocampal tissues was not altered (Fig. S1*B*). Furthermore, isolated microvascular fragments (Fig. S1*C*) from *S1pr1*^{iECKO} brain displayed normal mRNA expression of brain EC-specific genes (*Slco1c1*, *Slc2a1*, *Abcb1a*, *Mfsd2a*, and *Zic3*) (ref. 21; Fig. S1*D*) or other components of the NVU, smooth muscle cells (*Acta2*), pericytes (*Pdgfrb*), astrocytes (*Gfap*, *Aqp4*, and *Mfge8*), and perivascular macrophages (*Mrc1* and *Lyve1*) (ref. 25; Fig. S1*E*). Together, these results show that *S1pr1*^{iECKO} brain ECs undergo normal development, CNS-specific EC differentiation, and NVU development.

Inflammatory Gene Expression and Cognitive Function in Early Postnatally Deleted *S1pr1*^{iECKO} Mice. An increase in BBB permeability has been associated with neuroinflammation (26). For example, the mRNA expression of inflammatory cytokine genes including *Il1b*, *Tnfa*, and *Il6* increased (up to 40- to 60-fold) in multiple animal stroke models (27). We next examined inflammatory gene expression in the cortex and hippocampus of control and *S1pr1*^{iECKO} mice. However, there was no significant difference in the expression level of *Il1b*, *Tnfa*, and *Il6* between *S1pr1*^{iECKO} mice and controls (Fig. 2*C*). In addition, *S1pr1*^{iECKO} brains had no signs of perivascular reactive astrogliosis (3) (Fig. S3).

BBB disruption has also been associated with cognitive impairments (28, 29). Of note, chronic, but not acute, hypertension increases BBB leakage for small molecules, which causes cognitive impairment by enhancing exposure of angiotensin II to perivascular macrophage (30). Therefore, we asked whether deletion of endothelial *S1pr1* and after BBB opening can affect recognition memory. For this purpose, control and *S1pr1*^{iECKO} mice were tested for the novel object recognition (NOR) task, a paradigm that is commonly used to investigate recognition memory performance (31). In this behavioral test, we found that *S1pr1*^{iECKO} mice spent significantly less time in exploring a novel object than control mice (Fig. 2*D*), although the extent of the impairment was milder than the murine chronic hypertension models (10% vs. 20% reduction in novel object exploration time). Notably, *S1pr1*^{iECKO} mice did not show memory defects when endothelial *S1pr1* deletion was induced in the adult (Fig. 2*E*). Therefore, chronic defects in endothelial $S1P_1$ signaling that began at early postnatal period led to deficits in cognition memory.

Altered Subcellular Distribution of TJ Protein in *S1pr1*^{iECKO} Brain Microvessels. BBB is characterized by highly specialized TJs sealing the paracellular space between adjacent ECs and a low rate of transcytosis from the vessel lumen to the brain parenchyma (1–3). Size-selective BBB opening has been observed in mouse models where TJ genes, including the *Cldn5* encoding claudin-5 and/or the *Ocln* encoding occludin, were deleted or knocked down (32–34). Therefore, we sought to determine whether BBB opening in *S1pr1*^{iECKO} mice is associated with TJ protein modulation. To this end, we first compared the expression levels of major TJ proteins, claudin-5, occludin, and ZO-1, together with AJ protein, VE–cadherin, between control and *S1pr1*^{iECKO} mice. Examination of mRNA and protein expression levels in purified brain microvessels revealed that *S1pr1*^{iECKO}

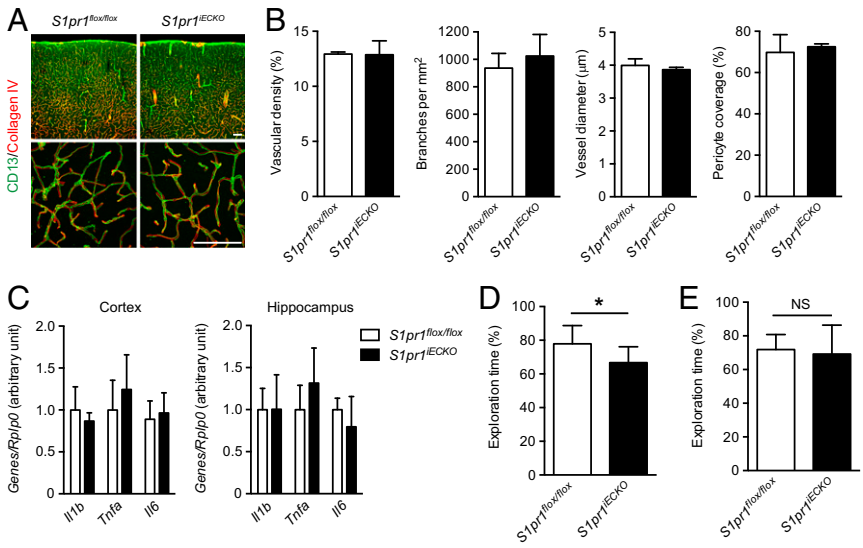

Fig. 2. Endothelial deletion of *S1pr1* in the neonatal period did not affect brain vascular development or induce inflammation, but is associated with cognitive impairment. (*A*) Representative confocal images of cerebral cortex from control ($S1pr1^{flox/flox}$) and $S1pr1^{iECKO}$ mice stained with collagen IV (basement membrane) and CD13 (pericyte). *A*, *Lower* shows high-power magnification images. (Scale bars: 100 μm.) (*B*) Quantification of cortical vascular density, branching, diameter, and pericyte coverage ($n = 3$). (*C*) qPCR analysis on the expressions for *Il1b*, *Il6*, and *Tnfa* in cerebral cortex and hippocampus ($n = 5$). (*D* and *E*) Assessment of recognition memory performance on control and $S1pr1^{iECKO}$ mice by NOR task when the deletion starts after birth (*D*) or in the adult (*E*). The exploration time of the novel objects was expressed in percent of both novel and familiar objects ($n = 11$, *D*; $n = 7$, *E*). Data are expressed as mean ± SD. $*P < 0.05$ (Student's *t* test). NS, nonsignificant.

mice showed normal expression levels for these TJ and AJ proteins (Fig. 3 *A* and *B*). TJs and AJs are linked to the cortical actin cytoskeleton, which controls the subcellular distribution and functions of these adhesive proteins (35). Because $S1P_1$ is a key regulator of endothelial actin cytoskeleton (10), we further examined the subcellular distribution of TJ and AJ proteins in the brain vasculature. For this purpose, subcellular distribution of TJ proteins was examined by immunofluorescence confocal

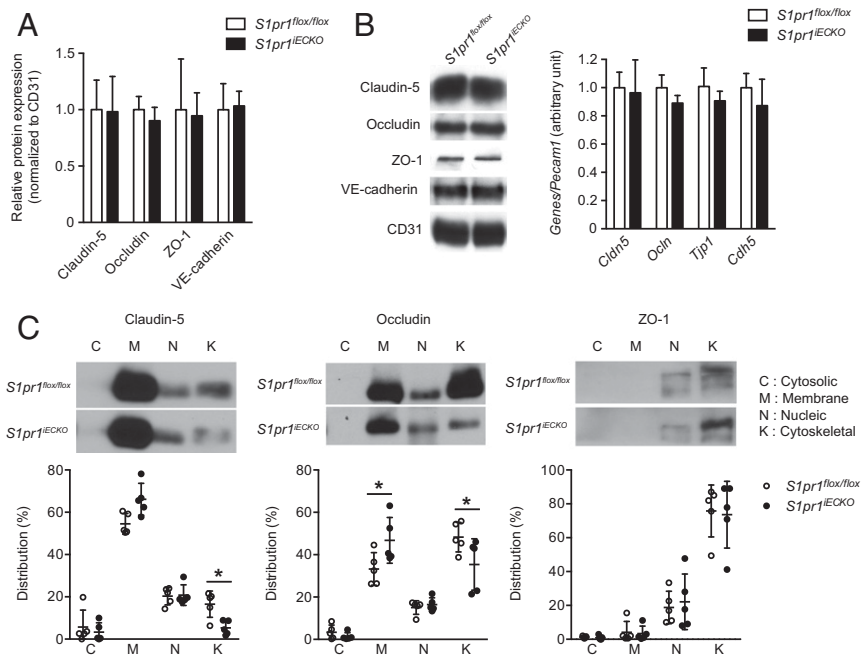

Fig. 3. Altered subcellular distribution of TJ proteins in brain microvessels of $S1pr1^{iECKO}$ mice. (*A*) qPCR analysis on the mRNA expression for TJ proteins *Cldn5*, *Ocln*, and *Tjp1* and AJ protein *Cdh5* in microvascular fragments from control ($S1pr1^{flox/flox}$) and $S1pr1^{iECKO}$ mice. Relative expression levels normalized to pan-EC marker *Pecam1* are shown ($n = 4$). (*B*) Representative immunoblot image (*Left*) with quantification (*Right*) of TJ proteins Claudin-5, Occludin, and ZO-1 and AJ protein VE-cadherin in control and $S1pr1^{iECKO}$ brain microvessels. Anti-CD31 antibody was used as a loading control and for the normalization in quantification ($n = 3$). (*C*) Subcellular distribution of TJ proteins Claudin-5, Occludin, and ZO-1 in control and $S1pr1^{iECKO}$ brain microvessels ($n = 5$). Representative immunoblot images (*C*, *Upper*) with quantification (*C*, *Lower*) are shown. The distribution of TJ proteins in each fraction represents percent of total (*C*, *Lower*). Data are expressed as mean ± SD. $*P < 0.05$ (one-way analysis of variance).

microscopy. However, we did not observe obvious differences in the TJ protein distribution in microvessels from control and *S1pr1*^{iECKO} brains (Fig. S4*A*). Next, we performed subcellular fractionation experiments using purified microvessels from the brain of control and *S1pr1*^{iECKO} mice. Irrespective of the genotypes, CD31 and VE–cadherin were exclusively detected in the membrane and cytoskeletal fractions, respectively (Fig. S5). Meanwhile, claudin-5 and occludin were detected in the membrane, nuclear, and cytoskeletal fractions. Higher expression of these TJ proteins was observed in the membrane fraction, but less expression was detected in actin cytoskeletal fraction in *S1pr1*^{iECKO} microvascular fragments compared with control mice (Fig. 3*C*). However, immunofluorescence confocal microscopy did not detect altered subcellular distribution of TJ proteins (Fig. S4*B*). These results suggest that the loss of *S1pr1* reduces cytoskeletal association of TJ proteins without gross changes in their expression level or localization in brain ECs, which may facilitate an increase in BBB permeability to small molecules.

Reversible and Size-Selective Opening of BBB by Pharmacological Targeting of S1P$_1$. Because *S1pr1* deletion induced a size-selective BBB opening, we next investigated whether S1P$_1$ inhibitors can open the BBB. For this purpose, we used the FDA-approved drug FTY720 (fingolimod), which targets all S1P receptors except S1P$_2$ (7). FTY720 is a prodrug that is phosphorylated in vivo to form FTY720-P, which works as functional antagonist for the S1P$_1$ by inducing its internalization and degradation (11, 36, 37). Indeed, three consecutive days of treatment with FTY720 successfully reduced the expression of S1P$_1$ in microvascular fragments (Fig. 4*A*). FTY720-treated wild-type mice showed higher brain accumulation of 1-kDa Alexa Fluor 555–cadaverine tracers, but not of the 10-kDa tracer, recapitulating the *S1pr1*^{iECKO} mice phenotype (Fig. 4 *B* and *C*). However, FTY720 treatment did not show any enhancement of 1-kDa Alexa Fluor 555–cadaverine extravasation to brain parenchyma in *S1pr1*^{iECKO} mice, indicating that the effect is S1P$_1$-dependent (Fig. 4*D*). Importantly, the BBB opening induced by FTY720 was reversible and was not observed at 7 d after the injection (Fig. 4*E*). Treatment with the S1P$_1$-selective functional antagonist NIBR-0213 (38) showed fivefold increase of 1-kDa Alexa Fluor 555–cadaverine accumulation in brain parenchyma at 6 h after injection, but not at 48 h after injection of NIBR-0213 (Fig. 4 *F* and *G*). Collectively, these results indicate that pharmacological targeting of S1P$_1$ reversibly increases the BBB permeability in a size-selective manner.

Discussion

The BBB is essential for the maintenance of brain homeostasis, while BBB dysfunction has been associated with numerous CNS diseases (1–3). Therefore, maintenance and restoration of normal BBB function is thought to be a potential therapeutic approach. Conversely, BBB is an impediment to drug delivery into the CNS. Therefore, a detailed understanding of the development and maintenance of BBB is of critical importance for the development of novel therapeutic approaches for many CNS diseases (4). In the present study, we examined the role of endothelial S1P$_1$ on BBB function using *S1pr1*^{iECKO} mice. We found that *S1pr1*^{iECKO} mice exhibit a small-molecule-selective BBB opening, without major signs of CNS inflammation or injury. Such a size-selective BBB opening could be attributed to changes in the subcellular localization of TJ proteins. Furthermore, we succeeded in reversibly and size-selectively opening the BBB by pharmacological blockage of S1P$_1$.

Numerous studies have examined BBB development or maintenance (2); however, there is limited evidence of size-selective disruption of BBB in mice. For example, *Cldn5* knockout (32), as well as knockdown of both *Cldn5* and *Ocln* (33, 34), results in

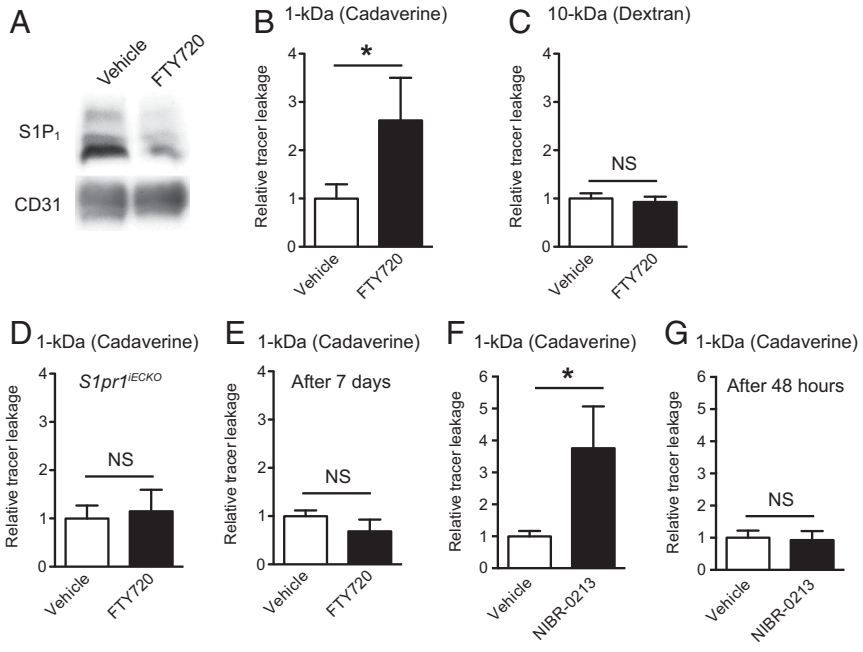

Fig. 4. Pharmacological targeting of S1P$_1$ increased brain tracer extravasation in a size-selective and reversible manner. (*A*) Immunoblot analysis of S1P$_1$ in microvascular fragments from vehicle- or FTY720-treated (5 mg/kg for three consecutive days) mice. CD31 expression is shown as a loading control. (*B* and *C*) Quantification of extravasated 1-kDa Alexa Fluor 555–cadaverine (*B*) and 10-kDa dextran–TMR (*C*) in vehicle- or FTY720-treated mice. (*D*) Quantification of 1-kDa Alexa Fluor 555–cadaverine brain leakage in vehicle- or FTY720-treated *S1pr1*^{iECKO} mice. (*E*) Quantification of extravasated 1-kDa Alexa Fluor 555–cadaverine in vehicle- or FTY720-treated mice at 7 d after treatment. (*F* and *G*) Quantification of extravasated 1-kDa Alexa Fluor 555–cadaverine in vehicle-treated or NIBR-0213–treated (30 mg/kg) mice at 6 h (*F*) or 48 h (*G*) after the treatment. Data are expressed as mean ± SD. $n = 3$ or 4. $^*P < 0.05$ (Student's *t* test). NS, nonsignificant.

enhanced BBB permeability to small molecules. These reports have highlighted that small-molecule transport through the BBB may occur via the paracellular route. Interestingly, the molecular size threshold for increased permeability observed in *S1pr1*^{iECKO} mice (3–10 kDa) is similar to that in *Cldn5* and *Ocln* double knockdowns (34). Thus, inhibition of $S1P_1$-regulated TJ protein function in brain EC may allow small molecules to enter the brain parenchyma.

Very recently, two other molecules, lipolysis-stimulated lipoprotein receptor (39) and GPR116 (40), were shown to regulate BBB permeability in a size-selective manner. Although TJ morphology did not show major alterations in these models (39, 40), it is still conceivable that $S1P_1$ may regulate BBB function by cooperating with these molecules. Indeed, $S1P_1$ and GPR116 are both EC-enriched GPCRs, and may contribute to BBB maintenance through common mechanisms.

As a barrier-enhancing GPCR, $S1P_1$ has been reported to regulate AJ by regulating VE–cadherin distribution in cultured ECs (10, 41). Although our biochemical approach did not show any changes in VE–cadherin subcellular distribution in *S1pr1*^{iECKO} mice, alteration of the AJ structure or function may also be involved in the increased BBB leakage in these mice.

The molecular mechanism by which loss of $S1P_1$ alters the localization of TJ proteins in brain ECs is still unknown. One possibility is that continuous activation of $S1P_1$ might be essential for cortical actin formation in brain ECs, which could directly facilitate proper maintenance of TJ protein complexes (35). Importantly, the $S1P_1$/Rac pathway strongly induces cortical actin rearrangement by regulating actin-associated proteins, cortactin and myosin light chain kinase, in cultured ECs (10). Another possibility is that $S1P_1$ regulates phosphorylation of TJ proteins. Multiple phosphorylation sites have been reported in claudin-5, occludin, and ZO-1 (42), which have been linked to both increases and decreases in their interaction to actin cytoskeleton (43). Notably, these phosphorylation sites are targets of c-Src, FAK, PI3Ks, Rho kinases, and PKCs (42), which can be modulated by $S1P_1$ signaling. Further studies are needed to examine whether TJ phosphorylation is altered in *S1pr1*^{iECKO} mice, and, if so, to assess which signaling pathways are used.

Size-selective leakage of BBB observed in *S1pr1*^{iECKO} mice may impact initiation or progression of CNS diseases. High levels (~1 μM) of S1P are found in blood, and more than half of plasma S1P is associated with high-density lipoprotein (HDL) (44). Importantly, lower plasma concentrations of HDL were reported to be associated with dementia (45). Considering that BBB leakage for small-size molecules (angiotensin II) can lead to cognitive defects (30), attenuated HDL/$S1P_1$-dependent tightening of the BBB may be a risk factor for dementia. A recent study also demonstrated that BBB disruption is selective for small-size molecules at the early phase of murine ischemic brain injury (46). This initial size-selective BBB disruption was attributed to actin cytoskeletal changes (46), which is a likely mechanism of BBB disruption in *S1pr1*^{iECKO} mice, as discussed above. Importantly, $S1P_1$ agonists may be protective in ischemic stroke (9), and an anticoagulant protein S displayed a protective role in hypoxic/ischemic BBB disruption in a $S1P_1$-dependent manner (47). Together, these observations raise the possibility that brain endothelial $S1P_1$ may have a protective role in ischemic brain injury or dementia.

Endothelial $S1P_1$ may be one of the key regulators of homeostatic BBB function. Tonic activation of $S1P_1$ in brain ECs from the luminal side may tighten the paracellular barrier and promote BBB function. In addition, $S1P_1$ activity may also be regulated from the abluminal side by circulating S1P. In the lymphoid organs, multiple perivascular cellular components maintain local perivascular S1P gradients, which are important for immune cell trafficking (44). Recent studies suggest the highly dynamic nature of BBB during the sleep–awake cycle (48). The plasticity of the BBB seems to be important to facilitate both the protection of brain from blood-derived toxins and the elimination of deleterious byproducts of brain metabolism. Because brain capillary endothelium is surrounded by other cellular components of NVU, the potential perivascular local supply of S1P might facilitate $S1P_1$-dependent BBB maintenance by cooperating with circulatory S1P.

Our study also suggests that targeting endothelial $S1P_1$ could be a promising approach for the delivery of therapeutic agents to the CNS. Many attempts have been made to bypass the BBB for CNS drug delivery (4). However, massive disruption of the BBB could have damaging consequences for the CNS (4). Therefore, reversible and limited opening of the BBB would be an ideal strategy for CNS drug delivery. Indeed, using FTY720 and NIBR-0213, we were able to reversibly open the BBB. The size-selective property of BBB opening by targeting $S1P_1$ would also offer the safe CNS delivery of compounds by avoiding severe brain inflammation or edema that could be driven by the transfer of blood-borne macromolecules into the brain parenchyma, such as fibrinogen. This notion is further supported by the observation that *S1pr1*^{iECKO} mice did not show any signs of inflammation or gliosis in brain. Indeed, *S1pr1*^{iECKO} mice did not show memory defects if endothelial *S1pr1* was deleted at adult stages.

Notably, it is reported that $S1P_1$-agonism reduces P-glycoprotein (P-gp) transport activity in rodent in situ perfusion experiments (49). In that study, FTY720 was shown to increase brain accumulation of the drugs by its agonistic activity. Furthermore, the authors found unaltered brain distribution of sucrose by either $S1P_1$ agonist or antagonist, suggesting that TJ-mediated paracellular BBB permeability may not be regulated by $S1P_1$. Although the reasons for this discrepancy remain unclear, differences in chemical properties of tracers (cadaverine or dextran vs. sucrose), model system (awake mouse vs. in situ perfusion), or ligand administration route (gavage vs. carotid infusion) may have played a role. Future studies testing different classes of tracers including P-gp substrates on *S1pr1*^{iECKO} mice would help provide a better understanding of the different factors determining the BBB functional characteristics.

In summary, we have demonstrated that endothelial $S1P_1$ regulates BBB permeability in a size-dependent manner. Furthermore, we have shown that pharmacological targeting of $S1P_1$ induces a reversible opening of the BBB, which may be of potential therapeutic value for the safe delivery of drugs into the CNS. Further investigations into the contribution of $S1P_1$ in other NVU components on the development and maintenance of BBB would yield important information for the future therapeutic application of $S1P_1$ modulators on a variety of CNS diseases.

Materials and Methods

Mouse Strains. Mice were housed in individual ventilated cages in a temperature-controlled facility with a 12-h light/dark cycle at Weill Cornell Medical College. EC-specific *S1pr1* knockout mice (*S1pr1*$^{flox/flox}$ *Cdh5–Cre–ER*^{T2}; *S1pr1*^{iECKO}) were generated as described (12, 13, 16, 17). Mice were treated with tamoxifen by oral gavage (50 μg/d) for the first 3 d after birth and used for the experiments at the age of 10–16 wk. For the adult deletion experiments, 8-wk-old mice were treated with tamoxifen by oral gavage (100 μg per gram of body weight) for three consecutive days and used for the experiments 4 wk after last injection of tamoxifen. *S1pr1*$^{flox/flox}$ mice without the *Cdh5–Cre–ER*^{T2} gene were treated with tamoxifen in the same way as *S1pr1*^{iECKO} mice and used as control mice (*S1pr1*$^{flox/flox}$). All experiments were performed in male mice. All animal experiments were approved by the Weill Cornell Institutional Animal Care and Use Committee.

Tracer Injection Experiments. Brain tracer leakage experiments were performed as described (40, 50). Mice (10–12 wk of age) were injected in the tail vein with Alexa Fluor 555–cadaverine (6 μg/g; Invitrogen), 3-kDa dextran–TMR (10 μg/g; Invitrogen), 10-kDa dextran–TMR (15 μg/g; Invitrogen), or 70-kDa dextran–TMR (100 μg/g; Invitrogen) dissolved in saline. After 2 h (for Alexa Fluor 555–cadaverine or 3-kDa dextran–TMR), 4 h (for 10-kDa dextran–TMR), or 16 h (for 70-kDa dextran–TMR), mice were anesthetized and perfused for 7 min with ice-cold PBS (pH 7.4), and brains were removed. After dissection, the cortex was weighed and homogenized with 1% Triton

X-100 in PBS. Cortical lysates were centrifuged at 12,000 × *g* for 20 min at 4 °C, and the supernatant was used to quantify fluorescence (excitation/emission 540/590 nm; SpectraMax M2e; Molecular Devices). The relative fluorescence values were normalized with cortical weights.

Retinal tracer leakage experiments were performed as described (51). Under deep isoflurane anesthesia, 3-kDa dextran–TMR (50 μg/g) was injected intravenously. After 10 min, the chest cavity was opened, and mice were perfused for 7 min with ice-cold PBS. After perfusion, retinas were removed and homogenized in distilled water. The extract was processed through a 30,000-molecular-weight filter (Amicon Ultra-0.5 mL; Millipore) at 13,000 × *g* for 10 min. The fluorescence in each 300-μL sample was measured (excitation/emission 540/590 nm; SpectraMax M2e).

Brain Microvascular Fragments. Brain microvascular fragments were prepared as described (52, 53) with minor modifications (see details in *SI Materials and Methods*).

qPCR Analysis, Immunoblot Analysis, and Immunohistochemistry. RNA isolation, RT-qPCR analysis, preparation of total lysates or subcellular fractions, Western blotting, and immunofluorescence experiments were performed as described in *SI Materials and Methods*.

NOR. The NOR task was conducted as described (30) (see details in *SI Materials and Methods*).

Drug Treatment. FTY720 and NIBR-0213 are kind gifts from Novartis. To examine the effect of FTY720, mice were administered 5 $mg \cdot kg^{-1} \cdot d^{-1}$ FTY720 or vehicle (water) via oral gavage continuously for three consecutive days. These mice were used for the tracer injection experiments 1 or 7 d after last injection of FTY720. For NIBR-2013 experiments, mice were treated with 60 mg/kg NIBR-0213 or vehicle [30% (vol/vol) PEG/phosphate buffer (pH 7.4)] via oral gavage. The mice were used for the tracer injection experiments 6 or 48 h after NIBR-0213 injection.

Statistical Analysis. Statistical analysis was performed by using two-tailed Student's *t* test or one-way analysis of variance with Bonferroni's multiple comparison test as described using Prism software (GraphPad). P values < 0.05 were considered statistically significant. All results are expressed as the mean ± SD.

ACKNOWLEDGMENTS. We thank Steven Swendeman, Akira Ito, Nichole Chang (Weill Cornell Medicine), Christer Betsholtz, Bongnam Jung (Uppsala University), Annika Keller, and Josephin Wagner (University Hospital Zurich) for technical help and advice. This work is supported by NIH Grants HL89934, HL117798, and HL135821 (to T.H.), NS89323, NS95441, and NS100447 (to C.I.), and HL094465 (to T.S.); a Fondation Leducq Transatlantic Network Grant (to T.H., C.I., and T.S.); and American Heart Association Grants GIA12GRNT12050110 (to T.S.) and 15SDG22760007 (to G.F.). K.Y. was supported by the Japan Society for the Promotion of Science.

1. Zhao Z, Nelson AR, Betsholtz C, Zlokovic BV (2015) Establishment and dysfunction of the blood-brain barrier. *Cell* 163:1064–1078.
2. Chow BW, Gu C (2015) The molecular constituents of the blood-brain barrier. *Trends Neurosci* 38:598–608.
3. Obermeier B, Daneman R, Ransohoff RM (2013) Development, maintenance and disruption of the blood-brain barrier. *Nat Med* 19:1584–1596.
4. Banks WA (2016) From blood-brain barrier to blood-brain interface: New opportunities for CNS drug delivery. *Nat Rev Drug Discov* 15:275–292.
5. Pardridge WM (2005) The blood-brain barrier: Bottleneck in brain drug development. *NeuroRx* 2:3–14.
6. Proia RL, Hla T (2015) Emerging biology of sphingosine-1-phosphate: Its role in pathogenesis and therapy. *J Clin Invest* 125:1379–1387.
7. Brinkmann V, et al. (2010) Fingolimod (FTY720): Discovery and development of an oral drug to treat multiple sclerosis. *Nat Rev Drug Discov* 9:883–897.
8. Brunkhorst R, Vutukuri R, Pfeilschifter W (2014) Fingolimod for the treatment of neurological diseases-state of play and future perspectives. *Front Cell Neurosci* 8:283.
9. Sanchez T (2016) Sphingosine-1-phosphate signaling in endothelial disorders. *Curr Atheroscler Rep* 18:31.
10. Xiong Y, Hla T (2014) S1P control of endothelial integrity. *Curr Top Microbiol Immunol* 378:85–105.
11. Oo ML, et al. (2011) Engagement of $S1P_1$-degradative mechanisms leads to vascular leak in mice. *J Clin Invest* 121:2290–2300.
12. Jung B, et al. (2012) Flow-regulated endothelial S1P receptor-1 signaling sustains vascular development. *Dev Cell* 23:600–610.
13. Montrose DC, et al. (2013) $S1P_1$ localizes to the colonic vasculature in ulcerative colitis and maintains blood vessel integrity. *J Lipid Res* 54:843–851.
14. Christensen PM, et al. (2016) Impaired endothelial barrier function in apolipoprotein M-deficient mice is dependent on sphingosine-1-phosphate receptor 1. *FASEB J* 30:2351–2359.
15. Allende ML, Yamashita T, Proia RL (2003) G-protein-coupled receptor S1P1 acts within endothelial cells to regulate vascular maturation. *Blood* 102:3665–3667.
16. Blaho VA, et al. (2015) HDL-bound sphingosine-1-phosphate restrains lymphopoiesis and neuroinflammation. *Nature* 523:342–346.
17. Galvani S, et al. (2015) HDL-bound sphingosine 1-phosphate acts as a biased agonist for the endothelial cell receptor S1P1 to limit vascular inflammation. *Sci Signal* 8:ra79.
18. London A, Benhar I, Schwartz M (2013) The retina as a window to the brain-from eye research to CNS disorders. *Nat Rev Neurol* 9:44–53.
19. Whiteus C, Freitas C, Grutzendler J (2014) Perturbed neural activity disrupts cerebral angiogenesis during a postnatal critical period. *Nature* 505:407–411.
20. Wälchli T, et al. (2015) Quantitative assessment of angiogenesis, perfused blood vessels and endothelial tip cells in the postnatal mouse brain. *Nat Protoc* 10:53–74.
21. Ben-Zvi A, et al. (2014) Mfsd2a is critical for the formation and function of the blood-brain barrier. *Nature* 509:507–511.
22. Gaengel K, et al. (2012) The sphingosine-1-phosphate receptor S1PR1 restricts sprouting angiogenesis by regulating the interplay between VE-cadherin and VEGFR2. *Dev Cell* 23:587–599.
23. Ben Shoham A, et al. (2012) S1P1 inhibits sprouting angiogenesis during vascular development. *Development* 139:3859–3869.
24. Paik JH, et al. (2004) Sphingosine 1-phosphate receptor regulation of N-cadherin mediates vascular stabilization. *Genes Dev* 18:2392–2403.
25. Zeisel A, et al. (2015) Brain structure. Cell types in the mouse cortex and hippocampus revealed by single-cell RNA-seq. *Science* 347:1138–1142.
26. Engelhardt B, Ransohoff RM (2012) Capture, crawl, cross: The T cell code to breach the blood-brain barriers. *Trends Immunol* 33:579–589.
27. Lambertsen KL, Biber K, Finsen B (2012) Inflammatory cytokines in experimental and human stroke. *J Cereb Blood Flow Metab* 32:1677–1698.
28. Zlokovic BV (2011) Neurovascular pathways to neurodegeneration in Alzheimer's disease and other disorders. *Nat Rev Neurosci* 12:723–738.
29. Sagare AP, Bell RD, Zlokovic BV (2012) Neurovascular dysfunction and faulty amyloid β-peptide clearance in Alzheimer disease. *Cold Spring Harb Perspect Med* 2:a011452.
30. Faraco G, et al. (2016) Perivascular macrophages mediate the neurovascular and cognitive dysfunction associated with hypertension. *J Clin Invest* 126:4674–4689.
31. Leger M, et al. (2013) Object recognition test in mice. *Nat Protoc* 8:2531–2537.
32. Nitta T, et al. (2003) Size-selective loosening of the blood-brain barrier in claudin-5-deficient mice. *J Cell Biol* 161:653–660.
33. Campbell M, et al. (2008) RNAi-mediated reversible opening of the blood-brain barrier. *J Gene Med* 10:930–947.
34. Keaney J, et al. (2015) Autoregulated paracellular clearance of amyloid-β across the blood-brain barrier. *Sci Adv* 1:e1500472.
35. Spindler V, Schlegel N, Waschke J (2010) Role of GTPases in control of microvascular permeability. *Cardiovasc Res* 87:243–253.
36. Gräler MH, Goetzl EJ (2004) The immunosuppressant FTY720 down-regulates sphingosine 1-phosphate G-protein-coupled receptors. *FASEB J* 18:551–553.
37. Oo ML, et al. (2007) Immunosuppressive and anti-angiogenic sphingosine 1-phosphate receptor-1 agonists induce ubiquitinylation and proteasomal degradation of the receptor. *J Biol Chem* 282:9082–9089.
38. Quancard J, et al. (2012) A potent and selective S1P(1) antagonist with efficacy in experimental autoimmune encephalomyelitis. *Chem Biol* 19:1142–1151.
39. Sohet F, et al. (2015) LSR/angulin-1 is a tricellular tight junction protein involved in blood-brain barrier formation. *J Cell Biol* 208:703–711.
40. Niaudet C, et al. (2015) Gpr116 receptor regulates distinctive functions in pneumocytes and vascular endothelium. *PLoS One* 10:e0137949.
41. Lee MJ, et al. (1999) Vascular endothelial cell adherens junction assembly and morphogenesis induced by sphingosine-1-phosphate. *Cell* 99:301–312.
42. González-Mariscal L, Tapia R, Chamorro D (2008) Crosstalk of tight junction components with signaling pathways. *Biochim Biophys Acta* 1778:729–756.
43. Bazzoni G, Dejana E (2004) Endothelial cell-to-cell junctions: Molecular organization and role in vascular homeostasis. *Physiol Rev* 84:869–901.
44. Yanagida K, Hla T (2017) Vascular and immunobiology of the circulatory sphingosine 1-phosphate gradient. *Annu Rev Physiol* 79:67–91.
45. Vitali C, Wellington CL, Calabresi L (2014) HDL and cholesterol handling in the brain. *Cardiovasc Res* 103:405–413.
46. Shi Y, et al. (2016) Rapid endothelial cytoskeletal reorganization enables early blood-brain barrier disruption and long-term ischaemic reperfusion brain injury. *Nat Commun* 7:10523.
47. Zhu D, et al. (2010) Protein S controls hypoxic/ischemic blood-brain barrier disruption through the TAM receptor Tyro3 and sphingosine 1-phosphate receptor. *Blood* 115:4963–4972.
48. Keaney J, Campbell M (2015) The dynamic blood-brain barrier. *FEBS J* 282:4067–4079.
49. Cannon RE, Peart JC, Hawkins BT, Campos CR, Miller DS (2012) Targeting blood-brain barrier sphingolipid signaling reduces basal P-glycoprotein activity and improves drug delivery to the brain. *Proc Natl Acad Sci USA* 109:15930–15935.
50. Armulik A, et al. (2010) Pericytes regulate the blood-brain barrier. *Nature* 468:557–561.
51. Muranaka K, et al. (2006) Effects of peroxisome proliferator-activated receptor gamma and its ligand on blood-retinal barrier in a streptozotocin-induced diabetic model. *Invest Ophthalmol Vis Sci* 47:4547–4552.
52. Biegel D, Spencer DD, Pachter JS (1995) Isolation and culture of human brain microvessel endothelial cells for the study of blood-brain barrier properties in vitro. *Brain Res* 692:183–189.
53. Boulay AC, Saubaméa B, Declèves X, Cohen-Salmon M (2015) Purification of mouse brain vessels. *J Vis Exp* (105):e53208.